

## Article

# Jasmonates and Ethylene Shape Floridoside Synthesis during Carposporogenesis in the Red Seaweed *Grateloupia imbricata*

Pilar Garcia-Jimenez <sup>\*</sup>, Diana del Rosario-Santana  and Rafael R. Robaina 

Department of Biology, Faculty of Marine Sciences, Instituto Universitario de Investigación en Estudios Ambientales y Recursos Naturales i-UNAT, Universidad de Las Palmas de Gran Canaria, 35017 Las Palmas, Spain; diana.delrosario@ulpgc.es (D.d.R.-S.); rafael.robaina@ulpgc.es (R.R.R.)

\* Correspondence: pilar.garcia@ulpgc.es

**Abstract:** Floridoside is a galactosyl-glycerol compound that acts to supply UDP-galactose and functions as an organic osmolyte in response to salinity in Rhodophyta. Significantly, the UDP-galactose pool is shared for sulfated cell wall galactan synthesis, and, in turn, affected by thallus development alongside carposporogenesis induced by volatile growth regulators, such as ethylene and methyl jasmonate, in the red seaweed *Grateloupia imbricata*. In this study, we monitored changes in the floridoside reservoir through gene expression controlling both the galactose pool and glyceride pool under different reproductive stages of *G. imbricata* and we considered changing salinity conditions. Floridoside synthesis was followed by expression analysis of *galactose-1-phosphate uridylyltransferase* (*GALT*) as UDP-galactose is obtained from UDP-glucose and glucose-1P, and through  $\alpha$ -*galactosidase* gene expression as degradation of floridoside occurs through the cleavage of galactosyl residues. Meanwhile, glycerol 3-phosphate is connected with the galactoglyceride biosynthetic pathway by glycerol 3-phosphate dehydrogenase (*G3PD*), monogalactosyl diacylglyceride synthase (*MGDGS*), and digalactosyl diacylglyceride synthase (*DGDGS*). The results of our study confirm that low *GALT* transcripts are correlated with thalli softness to locate reproductive structures, as well as constricting the synthesis of UDP-hexoses for galactan backbone synthesis in the presence of two volatile regulators and methionine. Meanwhile,  $\alpha$ -*galactosidase* modulates expression according to cystocarp maturation, and we found high transcripts in late development stages, as occurred in the presence of methyljasmonate, compared to early stages in ethylene. Regarding the acylglyceride pool, the upregulation of *G3PD*, *MGDGS*, and *DGDGS* gene expression in *G. imbricata* treated with MEJA supports lipid remodeling, as high levels of transcripts for *MGDGS* and *DGDGS* provide membrane stability during late development stages of cystocarps. Similar behavior is assumed in three naturally collected thalli development stages—namely, fertile, fertilized, and fertile—under 65 psu salinity conditions. Low transcripts for  $\alpha$ -*galactosidase* and high for *G3PD* are reported in infertile and fertilized thalli, which is the opposite to high transcripts for  $\alpha$ -*galactosidase* and low for *G3PD* encountered in fertile thalli within visible cystocarps compared to each of their corresponding stages in 35 psu. No significant changes are reported for *MGDGS* and *DGDGS*. It is concluded that cystocarp and thallus development stages affect galactose and glycerides pools with interwoven effects on cell wall polysaccharides.

**Keywords:** ethylene; floridoside; galactose-1-phosphate uridylyltransferase;  $\alpha$ -galactosidase; jasmonates; red seaweed; sulfated galactans



**Citation:** Garcia-Jimenez, P.; del Rosario-Santana, D.; Robaina, R.R. Jasmonates and Ethylene Shape Floridoside Synthesis during Carposporogenesis in the Red Seaweed *Grateloupia imbricata*. *Mar. Drugs* **2024**, *22*, 115. <https://doi.org/10.3390/md22030115>

Academic Editors: Leonel Pereira and Rui Pedro Gonçalves Pereira

Received: 9 January 2024

Revised: 23 February 2024

Accepted: 26 February 2024

Published: 28 February 2024



**Copyright:** © 2024 by the authors. Licensee MDPI, Basel, Switzerland. This article is an open access article distributed under the terms and conditions of the Creative Commons Attribution (CC BY) license (<https://creativecommons.org/licenses/by/4.0/>).

## 1. Introduction

Red seaweeds synthesize sulfated galactans, such as carrageenan, as a main component of their cell walls, whilst they also store polysaccharides such as floridoside. Sulfated and stored polysaccharides are synthesized from the UDP-hexose pool, which supplies UDP-galactose units to lead the synthesis of the galactan backbone, i.e., sulfated polysaccharides, and to transfer units to glycerol 3-phosphate in order to form floridoside [1].



On the other hand, glycerol 3-phosphate (G3P) originates from dihydroxyacetone phosphate (DHAP) and is converted to glycerol by means of a phosphatase [13]. Glycerol has been reported as a carbon source for the growth and development of the red seaweed *G. imbricata*. Glycerol provoked a 400% increment in fresh weight and the formation of cell masses after spores were cultured in its presence [14]. Additionally, glycerol has been required for salinity acclimation in other algae [15]. Moreover, G3P connects with the galactoglyceride biosynthetic pathway (Figure 1). In particular, galacto-acylglycerides, of which monogalactosyl diacylglyceride (MGDG) and digalactosyl diacylglyceride (DGDG) are the most abundant, result from the galactosylation of a diglyceride utilizing UDP-galactose [16,17] (Figure 1). Interestingly, MGDG and DGDG participate in the acclimation process, synthesis pathways for plant growth regulators such as jasmonates [17], and changes in the cell membrane fluidity due to alterations in the acylglycerol pool [18].

In these tangled scenarios where sulfated and stored polysaccharides share a precursor (UDP-galactose), and where the synthesis of sulfated polysaccharides is affected by the S-source (reduced vs. oxidized) as well as volatile PGR synthesis through SAM (S-adenosyl methionine), we hypothesized that stored polysaccharides, such as floridoside, may also be affected by the S-source (methionine and SO<sub>4</sub>) and PGRs. Alterations in the floridoside-stored polysaccharide reservoir may be valued through two approaches. The first approach is the synthesis of a pool of hexoses, which forms galactosyl units, and the second is the synthesis of a reservoir of acylglyceride, which supplies the synthesis of glycerol 3-phosphate and favors the flexibility of cell membranes. Accordingly, our aim in this study was to characterize the expression of genes involved in supporting the UDP-galactose pool through synthesis by *GALT* and degradation of floridoside by  $\alpha$ -galactosidase, and those associated with the acylglyceride reservoir such as *glycerol 3-phosphate dehydrogenase (G3PD)*, *monogalactosyl diacylglyceride synthase (MGDGS)*, and *digalactosyl diacylglyceride synthase (DGDGS)*, during carposporogenesis—induced by ethylene and MEJA—in thalli of the red seaweed *Grateloupia imbricata*, cultured separately in the presence of methionine and SO<sub>4</sub>.

In addition, gene expression during three reproductive stages of *G. imbricata*, namely, infertile, fertilized, and fertile thalli, was evaluated while increasing the salinity from 35 psu to 65 psu, as *G. imbricata* is an intertidal seaweed. This study sets a benchmark for outlining the connection between the synthesis of sulfated and stored polysaccharides in red seaweeds. Our insights into the genetic mechanisms of the synthesis of valued polysaccharides will contribute to formulating the controlled exploitation of these renewable resources.

## 2. Results

### 2.1. Influence of Ethylene and Meja on Expression of Genes Involved in Floridoside Synthesis alongside Cystocarp Development

The expression of a gene involved in the synthesis of the pool of UDP-galactose, *galactose-1-phosphate uridylyltransferase (GALT)*, showed a diminution of the transcript number of *GALT* in thalli treated with ethylene (Figure 2A) and MEJA (Figure 2B) in the presence of methionine. Otherwise, the transcript numbers of  $\alpha$ -galactosidase in thalli treated with ethylene were significantly repressed compared to those of the control (Figure 2A).

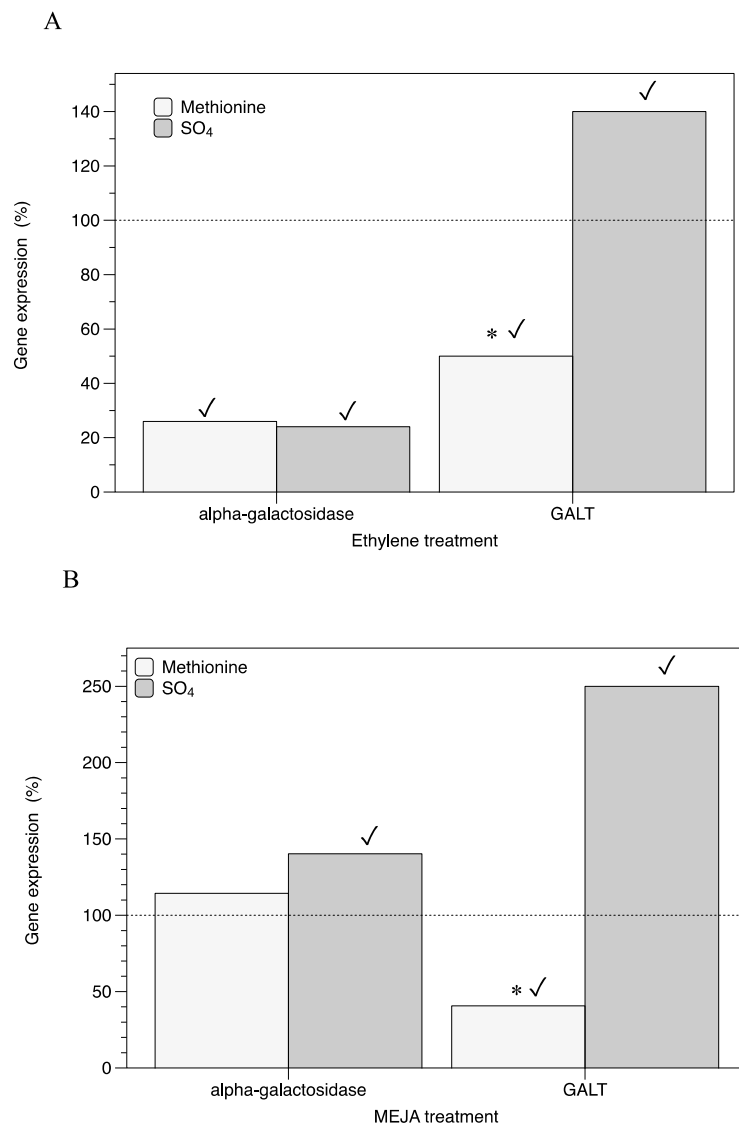


**Figure 2.** Expression of genes (*alpha-galactosidase* and *GALT*) that encode hexose pool (UDP-galactose) in thalli of *Grateloupia imbricata*. Expression was analyzed in thalli treated with methionine or MgSO<sub>4</sub> in (A) in ethylene-induced fertile thalli at an end time of 10 days (3 days S-source plus 7 days after ethylene treatment), and (B) in methyljasmonate (MEJA)-induced fertile thalli at an end time of 5 days (3 days S-source plus 2 days after MEJA treatment). Expressions (copies  $\mu\text{L}^{-1}$ ) are shown as percentages relative to expression in treated thalli at day 3 for methionine and for MgSO<sub>4</sub>, respectively (100%, dashed horizontal line). For methionine, thalli gene expression (i.e., 100%;  $p \leq 0.01$ ), *GALT* =  $120 \pm 1.3 \pm 1.8 \times 10^{-4}$ . For MgSO<sub>4</sub>, *GALT* =  $32 \pm 1.2 \times 10^{-5}$ . Gene expression of pooled samples (i.e., 100%) for *alpha-galactosidase* =  $15.4 \pm \pm 2.1 \times 10^{-5}$  was not affected by S-source. \* significant difference ( $p < 0.01$ ) between methionine and MgSO<sub>4</sub> treatment; ✓ differences between gene and the corresponding control. *GALT*, galactose-1-phosphate uridylyltransferase.

Regarding genes that encode proteins of the galactosyl-glycerol pool such as *G3PD*, *MGDGS*, and *DGDGS*, thalli cultured in ethylene showed significantly repressed expressions for *G3PD* and *DGDGS* in both S-sources (Figure 3). Meanwhile, in the presence of MEJA and methionine, *G3PD*, *MGDGS*, and *DGDGS* were always overexpressed (Figure 3B).

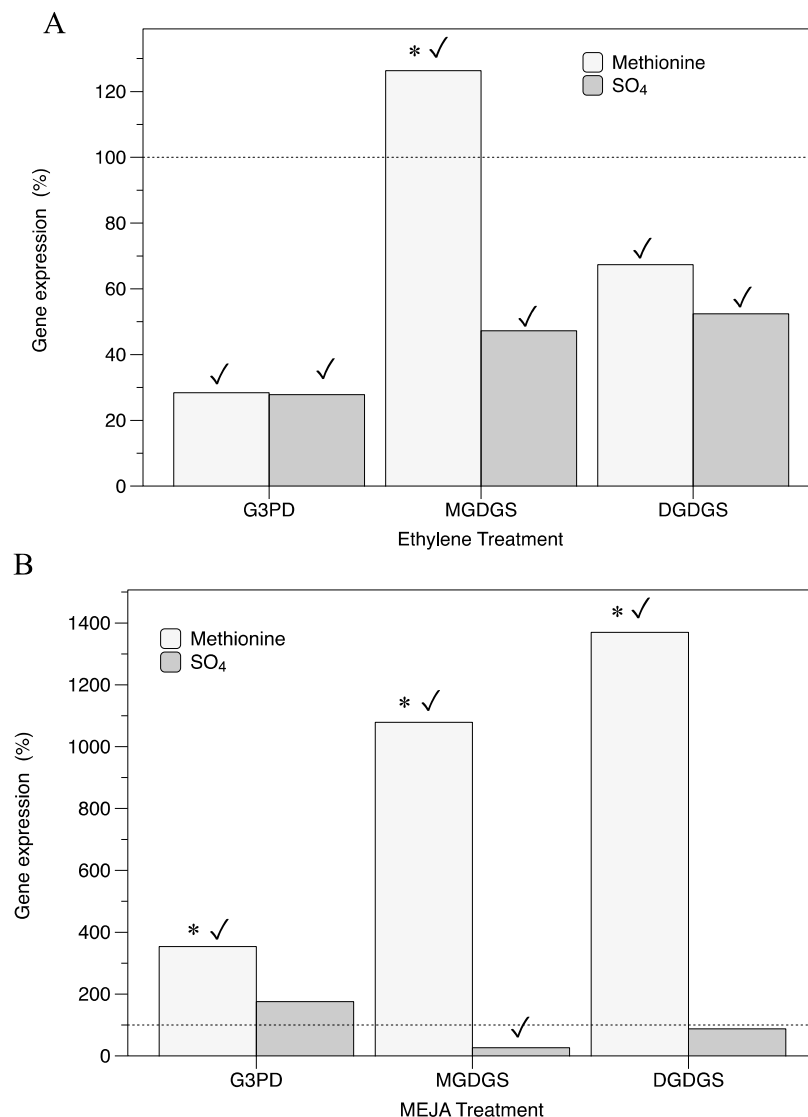


**Figure 3.** Expression of genes (*G3PD*, *MGDGS*, *DGDGS*) that encode galactosyl–glycerol pool in thalli of *Grateloupia imbricata*. Expression was analyzed in thalli treated with methionine or MgSO<sub>4</sub> in (A) ethylene-induced fertile thalli at an end time of 10 days (3 days S-source plus 7 days after ethylene treatment), and (B) in methyljasmonate (MEJA)-induced fertile thalli at an end time of 5 days (3 days S-source plus 2 days after MEJA treatment). Expressions (copies  $\mu\text{L}^{-1}$ ) are shown as percentages relative to expression in treated thalli at day 3 for methionine and for MgSO<sub>4</sub>, respectively (100%, dashed horizontal line). Gene expression of pooled samples (i.e., 100%),  $G3PD = 84.5 \pm 1.9 \times 10^{-5}$ ,  $MGDGS = 91 \pm 2.0 \times 10^{-4}$ , and  $DGDGS = 93.5 \pm 1.87 \times 10^{-4}$ . \* significant difference ( $p < 0.01$ ) between methionine and MgSO<sub>4</sub> treatment; ✓ differences between gene and the corresponding control.

## 2.2. Influence of Salinity on Gene Expression Involved in Floridoside Synthesis

Increasing the salinity from 35 psu to 65 psu provoked a downregulation of the expression of *GALT* in infertile, fertilized, and fertile thalli (Figure 4A). The gene encoding  $\alpha$ -galactosidase was only overexpressed (by nearly three times) in fertile thalli when compared to untreated thalli (35 psu; Figure 4A). Unlike the *G3PD* gene, which was overexpressed in infertile and fertilized thalli, no significant changes were found for the fertile stage, nor were any found for the *MGDGS* and *DGDGS* genes (Figure 4B).

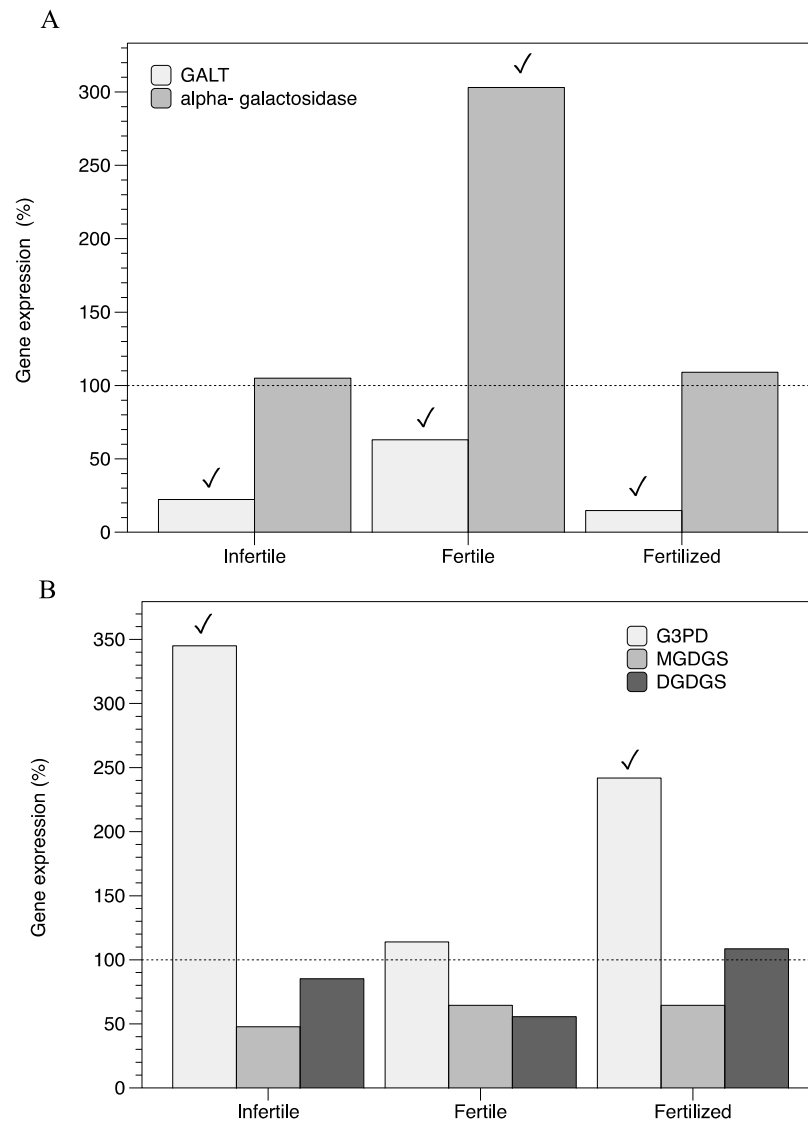


**Figure 4.** Expression of genes that encode (A) hexose pool (*alpha-galactosidase* and *GALT*) and that encode (B) galactosyl–glycerol pool (*G3PD*, *MGDGS*, *DGDGS*) under high-salinity conditions (65 psu) in three reproductive stages of thalli of *Grateloupia imbricata* (fertile, fertilized, and infertile thalli). Expressions (copies  $\mu\text{L}^{-1}$ ) are shown as percentages relative to expression in treated thalli at 35 psu (100%, dashed horizontal line). Thalli gene expression (i.e., 100%) *alpha-galactosidase* =  $63.22 \pm 10^{-3}$ , *GALT* =  $296.44 \pm 2.50 \times 10^{-3}$ , *G3PD* =  $48.01 \pm 2.7 \times 10^{-3}$ , *MGDGS* =  $88 \pm 3.1 \times 10^{-4}$ , and *DGDGS* =  $83.33 \pm 0.5 \times 10^{-4}$ . *GALT*, galactose-1-phosphate uridylyltransferase; *G3PD*, glycerol 3-phosphate dehydrogenase; *MGDGS*, monogalactosyl diacylglyceride synthase; *DGDGS*, digalactosyl diacylglyceride synthase. ✓ differences between gene expression at 65 psu and gene expression at 35 psu.

### 3. Discussion

Floridoside, a galactosyl–glycerol-stored polysaccharide of red seaweed, is formed through the conjugation of UDP-galactose and glycerol. Furthermore UDP-galactose, resulting from floridoside's breakdown by  $\alpha$ -galactosidase, contributes to the UDP-hexose pool required for the synthesis of sulfated polysaccharides. Hence, floridoside can act as a dynamic carbon reservoir that can be utilized for polysaccharide biosynthesis. Also, it has been reported that stored polysaccharides play a role in the life cycle [8] and salinity acclimation of seaweeds [19]. Therefore, the formation and degradation of floridoside could be interwoven with sulfated polysaccharides, as carrageenan biosynthesis is also dependent on the hexose pool and reproductive stages of red seaweeds [3,4]. Furthermore, it is relevant

that *GALT* expression has been associated with fluctuations in cell wall galactans in the red seaweed *Gracilaria changii* [20] whilst *GALT* expression has also accompanied cystocarp development from induced fertile thalli of *G. imbricata* treated with methionine (Figure 2). Accordingly, the reduced expression of *GALT*, as a gene precursor of galactan synthesis, has been explained by the contribution of methionine to a pool of sulfur organic compounds in algae, which will affect the expression levels of the genes encoding proteins responsible for the conversion of glucose 6P to 1P by PGM and the transformation to UDP-galactose by *GALT* [3,4]. Thus, *GALT* expression is downregulated in ethylene-induced fertile thalli with cystocarps in the early development stage (Figure 2A), as well as when late cystocarp development stages are reached in the presence of MEJA (Figure 2B). Unlike ethylene, MEJA induced rapid cystocarp maturation and spore release in as little as 48 h in *G. imbricata* thalli [21]. This is in concordance with a previous report, where a *GALT* transcript decrease was correlated with thalli softness, serving to locate reproductive structures, i.e., cystocarps [3,4], as well as constricting the synthesis of UDP-hexoses for galactan backbone synthesis. In the opposite of the case for  $\text{SO}_4$ , the reduced expression of *GALT* in methionine could be also explained by a synergistic effect, as methionine is used to synthesize S-methyl methionine (SMM) and S-adenosyl methionine (SAM), whereas SAM is a pivotal compound for ethylene synthesis and a donor of methyl groups for methyl jasmonate synthesis from jasmonic acid [22].

Otherwise, a reduction in  $\alpha$ -galactosidase gene expression in response to a volatile growth regulator may relate to restrained stored polysaccharide mobilization in ethylene-induced fertile thalli (Figure 2A). Early-stage cystocarps in ethylene-induced fertile thalli are encountered 7 days after treatment and continue progressing in maturity until spore release. Hence, thalli softness is still required to locate completely mature cystocarps, which increase in size at that time. Conversely, a significant increase in  $\alpha$ -galactosidase expression in MEJA (by more than 40% compared to the control) (Figure 2B) would indicate that galactosyl residues could be used to regenerate thalli through cell wall biosynthesis and somehow also prevent thallus injuries as the cystocarps would be completely open and the cell walls would be weakened [7]. Jasmonates are recognized as a disruptor of carrageenan synthesis in *G. imbricata* [4], leading to cystocarp dehiscence through the opening of cystocarps and the release of carpospores in as little as 48 h [7].

The synthesis of glycerol occurs with the formation of glycerol 3-phosphate and consequent dephosphorylation by glycerol 3-phosphate dehydrogenase (G3PD) and by a specific phosphatase [23]. While glycerol is a compound involved in the growth and development of *Grateloupia* spp. [14], glycerol 3-phosphate (G3P) seems to act as a regulator of plant signaling [24].

Upregulation of *G3PD* gene expression in MEJA-induced fertile thalli of *G. imbricata* could explain a supply of G3P for lipid synthesis, as G3PD links carbohydrates and lipid metabolism [25] (Figure 3B). Otherwise, glycerol has been reported as acting like a scavenger to adjust the reducing power in yeast [26], which would also contribute to shielding intermediates from MEJA signaling [21,27]. It is recognized that the synthesis of methyl jasmonate activates the oxidative metabolism of polyunsaturated fatty acids, generating ROSs (in the form of  $\text{O}_2$ ,  $\text{H}_2\text{O}_2$ , or  $\text{OH}^-$ ) and oxidized derivatives of polyunsaturated fatty acids [28,29]. This would imply that MEJA can provoke changes in the cell membrane fluidity with changes in acylglycerols such as monogalactosyl diacylglycerides (MGDG), and digalactosyl diacylglycerides [18] (DGDG). Indeed, changes in *MGDGS* and *DGDGS* gene expressions indicate the remodeling of cell membranes and allow us to infer that the synthesis of acylglycerols occurs differentially in fertile thalli in the presence of MEJA plus methionine (Figure 3B). The presence of different transcript levels associated with genes encoding lipid remodeling, such as for *MGDGS* and *DGDGS*, has been reported concomitant to differences in tissues [30,31]. This means that in the case of MEJA-induced fertile thalli of *G. imbricata*, high levels of transcripts for *DGDGS* support membrane stability as cystocarps are recognized in a late development stage compared to those in ethylene-induced fertile thalli, where only *MGDGS* is overexpressed (Figure 3A,B). Additionally, these significant

gene expression levels in the presence of MEJA and methionine, when compared to those from thalli in the presence of an oxidized S-source, such as  $\text{SO}_4$  (Figure 3B), potentially reveal that ROSs will oxidize excess methionine and form methionine sulfoxide species, which, in turn, can also act on the ROS repository [32]. Likewise, an ethylene double bond will allow this olefin to be easily converted into a range of reactive intermediates [33] and, together with those, methionine provokes fluctuations in the galactosyl–diacyl–glycerol reservoir [18] (Figure 3A).

Together with a likely modulation of the redox state owing to a volatile growth regulator, a scenario of changing osmolarity could also activate *G3PD* in order to constrain an increase in external salinity [34–36]. Mechanisms of osmoacclimation have been reported in several *Gracilaria* species as occurring through low-molecular-weight organic solutes, such as galactosyl–glycerols, which are accumulated in hypersaline conditions [37–39]. This may justify why *G3PD* was overexpressed in high-salinity-acclimatized thalli of *G. imbricata*, as thallus acclimation transitioned from 35 psu to 65 psu (Figure 4B). Moreover, *Grateloupia imbricata*, an intertidal red seaweed subjected to extreme changes in salinity, irradiance, and temperature, responds to glycerol, which we know as it is successfully used for heterotrophic growth of *G. imbricata* (formerly *G. doryphora*) [14]. Additionally, the expression of the  $\alpha$ -galactosidase gene, encoding the floridoside-degrading protein, is constant in a high-salinity situation in infertile and fertilized thalli (Figure 4A). In contrast, in fertile thalli, high transcripts of  $\alpha$ -galactosidase (Figure 4A) and unaltered *G3PD* (Figure 4B) could point to the cleavage of galactosyl residues from the floridoside reservoir to refurbish the cell wall of thalli with mature cystocarps. In higher plants, galactosidase activity is associated with a reduction in the level of galactosyl residues occurring in ripening seeds and different profiles have been reported of gene expression for  $\alpha$ -galactosidase in several tissues during the maturation and germination of seeds [40]. In red seaweeds, differential behavior for stored polysaccharides seems to occur according to the development stages of thalli, namely, infertile, fertile, and fertilized thalli. Thus, floridoside is accumulated in infertile and fertilized (i.e., non-visible cystocarps; high expression for *G3PD* and low for  $\alpha$ -galactosidase; Figure 4A,B) and degraded in fertile thalli (i.e., visible and late-mature cystocarps; low expression for *G3PD* and high for  $\alpha$ -galactosidase; Figure 4A,B), all in order to render galactosyl units available for the synthesis and restoration of the cell wall during the reproduction process of red seaweeds.

In conclusion, the synthesis and degradation of floridoside are interwoven with sulfated polysaccharides, serving to refurbish thalli according to the development stages of the red seaweed. This implies balanced gene expression through the downregulation of hexose pool transcripts (i.e., no units for the galactan backbone) to soften the cell wall and upregulation of those in charge of sustaining the galactosyl–glycerol pool to support fluidity and stabilization of cell membranes during late events of the carposporogenesis of *G. imbricata* induced by volatile growth regulators. Moreover, floridoside accumulation seems to be controlled for the reproductive stages of *G. imbricata* rather than salinity changes, as mobilization of the hexose pool is assumed during changes in  $\alpha$ -galactosidase gene expression alongside the three development stages of thalli, which transition as infertile, fertilized, and fertile thalli.

Understanding the gene mechanisms responsible for driving floridoside accumulation and degradation and for cell membrane flexibility during the reproductive events of red seaweeds, presents a unique opportunity to further our control of the biosynthesis of carrageenan, which is used as a marine source in diverse industries.

## 4. Materials and Methods

### 4.1. Plant Material and Culture Conditions

Infertile, fertile, and fertilized thalli from the carragenophytic *G. imbricata* were collected along the northeast coast of Gran Canaria in the Canary Islands.

Concerning the evaluation of the role of a plant growth volatile regulator on floridoside synthesis and considering the role of the S-source in polysaccharide synthesis [3,4,41],

infertile thalli were placed in 500 mL vessels (3 g per vessel) and cultivated separately, either with a reduced source of S such as methionine (10 mM) or oxidized as magnesium sulfate (1.6 mM) for 3 days. Then, infertile thalli were sprayed three times with a solution of 100  $\mu\text{M}$  MEJA (Sigma Co., St Louis, MO, USA) in 0.01% (*v/v*) ethanol in an autoclaved seawater solution [21] to elicit cystocarps. The thalli were kept for 1 h under a light source of 50  $\mu\text{mol photons m}^{-2} \text{s}^{-1}$  and continued to be cultivated for 48 h (henceforth, MEJA-induced fertile thalli with a late development stage of cystocarps; Figure 5).

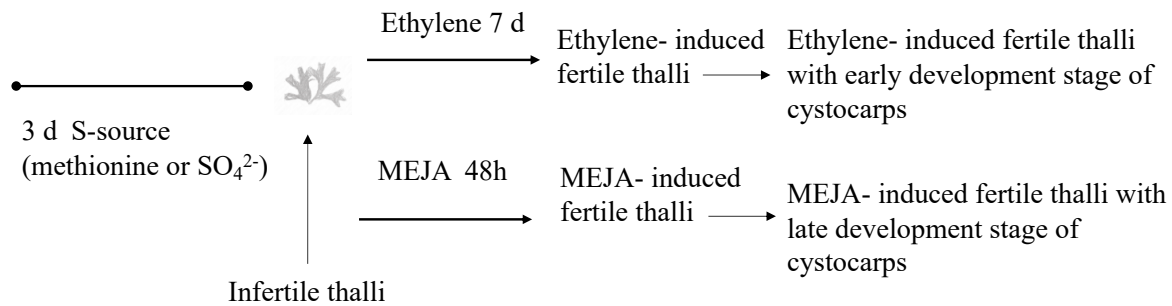


**Figure 5.** Scheme showing timeline for determination of gene expression (thin arrow) under ethylene and methyl jasmonate (MEJA) action in *Grateloupia imbricata*. This is infertile thalli treated with methionine or  $\text{MgSO}_4$  for 3 days; ethylene-induced fertile thalli at an end time of 10 days (3 days S-source plus 7 days after ethylene treatment); and in MEJA-induced fertile thalli at an end time of 5 days (3 days S-source plus 2 days after MEJA treatment). Controls are thalli treated for 3 days with the corresponding S-source.

Also, we triggered infertile thalli to elicit cystocarps by applying ethylene [42] (99.9% purity, Carburros Metálicos SA, Barcelona, Spain) to the 500 mL sealed vessels for 15 min at a flow rate of 0.5  $\text{L min}^{-1}$ . The thalli continued to be cultivated for 7 days (henceforth, ethylene-induced fertile thalli with an early development stage of cystocarps; Figure 5).

Thallus development from infertile to induced fertile thalli was verified through the gene expression of *ornithine decarboxylase* (*ODC*), which acts as a reproduction marker gene in red seaweeds [7,21,42]. The *ODC* gene expression was always downregulated in fertile thalli (i.e.,  $2.45 \pm 0.15 \times 10^{-2}$  copies  $\mu\text{L}^{-1}$  in infertile thalli and  $0.99 \pm 0.05 \times 10^{-2}$  copies  $\mu\text{L}^{-1}$  in fertile thalli) [3].

In order to assay the effect of salinity on the synthesis of floridoside, thalli were acclimated at 35 psu for 3 days to avoid bias as *G. imbricata* is an intertidal seaweed. Then, thalli were placed separately into three aquaria at 65 psu for 1 h, allowing us to classify them into fertile thalli, which showed axes with cystocarps; fertilized thalli, which displayed axes without visible cystocarps from the same individual with axes with cystocarps; and infertile thalli, which showed no cystocarps (Figure 6). All thalli were maintained at  $20 \pm 2$   $^\circ\text{C}$  under an 18 h light ( $50 \mu\text{mol photons m}^{-2} \text{s}^{-1}$ ): 6 h dark photoperiod in a growth chamber.

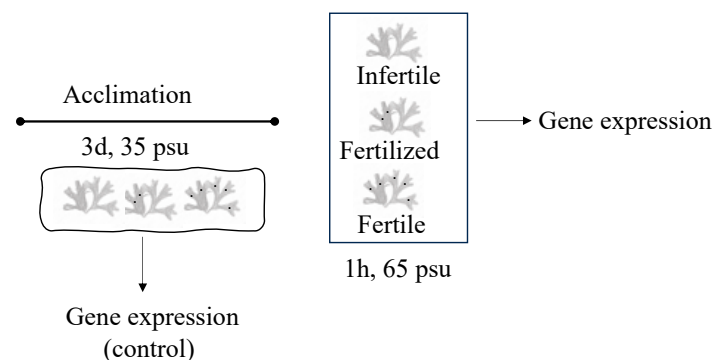


**Figure 6.** Scheme showing timeline for determination of gene expression (thin arrow) under high-salinity conditions in *Grateloupia imbricata*. Thalli were acclimated at 35 psu for 3 days (salinity control) and

then sorted according to reproductive stages (fertile, fertilized, and infertile thalli) and cultivated at 65 psu for 1 h.

#### 4.2. Influence of Ethylene and Methyl Jasmonate in Floridoside Synthesis

To value storage polysaccharide synthesis (i.e., floridoside synthesis), two approaches were deemed taking into consideration that floridoside synthesis is managed by 1) a pool of UDP-galactose and UDP-glucose and 2) a galactosyl–glycerol pool (Figure 1). Thus, the expression levels of *GALT*, which is in charge of forming UDP-galactose from galactose-1-P, and  $\alpha$ -*galactosidase*, which degrades floridoside, were measured. Also, genes encoding glycerol 3-phosphate dehydrogenase (G3PD, in charge of supplying glycerol 3-P) and those providing monogalactosyl diglyceride through *MGDG synthase* (*MGDGS*) and digalactosyl diglyceride by *DGDG synthase* (*DGDGS*) were analyzed as somehow they are involved in the synthesis of the galactosyl–glycerol pool (Figure 1).

All gene expression levels were valued in fertile thalli induced by MEJA and ethylene (Figure 5). Control samples (untreated and treated with each one of the S-sources) were processed in parallel. All samples were assayed in triplicate with two independent replicates for each experiment. At the end of the investigation period, samples of the thalli were frozen at  $-80\text{ }^{\circ}\text{C}$  until the isolation of RNA.

#### 4.3. Influence of Salinity Changes in Floridoside Synthesis

Transcripts of all genes detailed above were also measured in infertile, fertilized, and fertile thalli after acclimation for 3 days at 35 psu (control) and at 65 psu, to assess the salinity effect on floridoside synthesis (Figure 6). Samples and the control were assayed in triplicate with two independent replicates for each experiment. At the end of the investigation period, samples of the thalli were frozen at  $-80\text{ }^{\circ}\text{C}$  until the isolation of RNA.

#### 4.4. RNA Extraction

The total RNA was separately extracted from the upper-half regions (100 mg) of thalli using 1 mL of Tri-Reagent (Sigma, St. Louis, MO, USA), according to the manufacturer's instructions. The isolated RNA samples were individually suspended in 20  $\mu\text{L}$  of 1 M Tris-HCl (pH 8) and 0.5 M EDTA, and they were treated with DNase (1  $\text{Umg}^{-1}$ , Promega, Madison, WI, USA) to destroy contaminating DNA. The total RNA was quantified using a TrayCell cuvette and Beckman Coulter DU 530 spectrophotometer. Next, RNA extracted from each sample ( $\sim 1\text{ }\mu\text{g}$ ) was reverse transcribed in the presence of oligo (dT) and primers with randomly generated sequences from an iScript cDNA synthesis kit (Bio-Rad, Hercules, CA, USA). The reverse transcription procedure was carried out at  $25\text{ }^{\circ}\text{C}$  for 5 min,  $42\text{ }^{\circ}\text{C}$  for 30 min, and  $85\text{ }^{\circ}\text{C}$  for 5 min. The integrity of the cDNA was validated using a NanoDrop spectrophotometer (Thermo Fisher Scientific, Waltham, MA, USA). The products were kept at  $4\text{ }^{\circ}\text{C}$  until used.

#### 4.5. Droplet Digital PCR (ddPCR) Primers and Protocol Implementation

For quantification of each target transcript by ddPCR, QX200 ddPCR EvaGreen Supermix (Bio-Rad) was used according to the manufacturer's instructions. Briefly, for each sample, a PCR reaction mix (final volume 20  $\mu\text{L}$ ) was prepared containing 1.5  $\mu\text{L}$  of cDNA, 10  $\mu\text{L}$  of QX200 ddPCR Eva Green Supermix, and 0.22  $\mu\text{L}$  of each primer (10  $\mu\text{M}$ ), and then was loaded into a cartridge. Then, an oil droplet (70  $\mu\text{L}$ ) was loaded into each cartridge, and the cartridge was covered with a gasket. Each cartridge was individually introduced into the droplet generator, and finally, droplets of  $\sim 40\text{ }\mu\text{L}$  were transferred to the amplification plate. For each gene, three replicates were analyzed for each sample treated with MEJA and ethylene, acclimated to salinity, and we analyzed control samples accordingly. Primers for ddPCR were designed from cDNA sequences of the *G. imbricata* transcriptome (Table 1). PCR amplification was performed with a C1000 Touch Thermal Cycler (Bio-Rad) using the following conditions: an initial step at  $95\text{ }^{\circ}\text{C}$  for 5 min; followed by 40 cycles at  $95\text{ }^{\circ}\text{C}$  for 30 s, an experimentally determined annealing temperature for each gene for 1 min, and

72 °C for 45 s; then, a single step at 4 °C for 5 min; and a temperature ramping from 4 °C to 90 °C at a rate of 2 °C s<sup>-1</sup> for 5 min. After amplification, each sample was quantified using QuantaSoft v1.7.4 software (Bio-Rad). Data from merged wells (corresponding to each group of replicates) were retrieved, and the concentration of each group was given as the average number of transcript copies per µL.

**Table 1.** Sequences of the forward (F) and reverse (R) primers for each gene involved in synthesis of hexose pool (i.e., *alpha-galactosidase* and *galactose-1-phosphate uridylyl transferase (GALT)*), and in synthesis of galactosyl-glycerol pool, namely, *glycerol 3-phosphate dehydrogenase (G3PD)*, *monogalactosyl diacylglycerol synthase (MGDGS)*, and *digalactosyl diacylglycerol synthase (DGDGS)*.

Gene	Primer Name	Sequence (5'-3')
Synthesis of hexose pool		
<i>alpha-galactosidase</i>	AG-2468F	CTGTCAAGTTCCCGGATTCTC
	AG-2468R	TTCCTGCTGAAAGTCCCATTAG
<i>galactose-1-phosphate uridylyl transferase (GALT)</i>	G1PU-1681F	GTAGTAGATGCCTGGTGTGATG
	G1PU-1681R	CATATCTGGCCATGAGGATGAG
Synthesis of galactosyl-glycerol pool		
<i>glycerol 3-phosphate dehydrogenase (G3PD)</i>	G3PD-7275F	ACCTATCGGGTCTTCATTG
	G3PD-7275R	GGATGAGAACATGTCACCTAGAG
<i>monogalactosyl diacylglyceride synthase (MGDGS)</i>	MGS-2948F	TCCCGTTTAATCACTTCCCTTC
	MGS-2948R	ACTAAACGCGGTCTCAGTAATC
<i>digalactosyl diacylglyceride synthase (DGDGS)</i>	DGS-3637F	GTCCAATCCCAATCGAAGAGAG
	DGS-3637R	CTCAGCCAGACAATCCGATAA

#### 4.6. Data Analysis

Gene expression (transcript copies × µL<sup>-1</sup>) is reported as the mean ± standard deviation (SD). Statistical comparisons of concentrations were performed using R software (<https://www.r-project.org>; accessed on 6 July 2023). A one-way ANOVA followed by the post hoc tests Tukey HSD and Dunnett T3 was used to detect significant differences ( $p \leq 0.01$ ) between genes and their respective controls for each S-source (methionine and SO<sub>4</sub>).

**Author Contributions:** P.G.-J. conceived, designed, and wrote the manuscript. D.d.R.-S. conducted the experiments. P.G.-J. and R.R.R. discussed the manuscript. All authors have read and agreed to the published version of the manuscript.

**Funding:** General funding was provided from the Universidad de Las Palmas de Gran Canaria, and partially from Project TED2021-129249B-I00 funded by the Ministerio de Ciencia e Innovación (Spain).

**Data Availability Statement:** The original data presented in the study are included in the article; further inquiries can be directed to the corresponding author.

**Acknowledgments:** A fellowship from the Universidad de Las Palmas de Gran Canaria to D.d.R.-S. is acknowledged.

**Conflicts of Interest:** The authors declare that they have no conflicts of interest related to the present investigation.

## References

- Kremer, B.P.; Kirst, G.O. Biosynthesis of 2-OD-glycerol- $\alpha$ -D-galactopyranoside (Floridoside) in marine Rhodophyceae. *Plant Sci. Lett.* **1981**, *23*, 349–357. [[CrossRef](#)]
- Garcia-Jimenez, P.; Mantesa, S.R.; Robaina, R.R. Expression of genes related to carrageenan synthesis during carposporogenesis of the red seaweed *Grateloupia imbricata*. *Mar. Drugs* **2020**, *18*, 432. [[CrossRef](#)]
- del Rosario-Santana, D.; Robaina, R.R.; Garcia-Jimenez, P. Jasmonates disrupt carrageenan synthesis during carposporogenesis in the red seaweed *Grateloupia imbricata*. *Front. Mar. Sci.* **2023**, *10*, 1188493. [[CrossRef](#)]
- Del Rosario-Santana, D.; Robaina, R.R.; Garcia-Jimenez, P. S-Assimilation influences in Carrageenan Biosynthesis Genes during Ethylene-Induced Carposporogenesis in Red Seaweed *Grateloupia imbricata*. *Mar. Drugs* **2022**, *20*, 436. [[CrossRef](#)] [[PubMed](#)]

5. Garcia-Jimenez, P.; Robaina, R.R. *Systems Biology of Marine Ecosystems*; Kumar, M., Ralph, P., Eds.; Springer: Gewerbestrasse, Switzerland, 2017; Chapter 5; p. 99. [[CrossRef](#)]
6. Garcia-Jimenez, P.; Robaina, R.R. Effects of ethylene on tetrasporogenesis in *Pterocliadiella capillacea* (Rhodophyta). *J. Phycol.* **2012**, *48*, 710–715. [[CrossRef](#)] [[PubMed](#)]
7. Garcia-Jimenez, P.; Brito Romano, O.; Robaina, R.R. Occurrence of jasmonates during cystocarp development in the red alga *Grateloupia imbricata*. *J. Phycol.* **2016**, *52*, 1085–1093.
8. Yu, Y.; Jia, X.; Wang, W.; Jin, Y.; Liu, W.; Wang, D.; Mao, Y.; Xie, C.; Liu, T. Floridean starch and floridoside metabolic pathways of *Neoporphyra haitanensis* and their regulatory mechanism under continuous darkness. *Mar. Drugs* **2021**, *19*, 664. [[CrossRef](#)] [[PubMed](#)]
9. Barbier, G.; Oesterhelt, C.; Larson, M.D.; Halgren, R.G.; Wilkerson, C.; Garavito, R.M.; Benning, C.; Weber, A.P. Comparative genomics of two closely related unicellular thermo-acidophilic red algae, *Galdieria sulphuraria* and *Cyanidioschyzon merolae*, reveals the molecular basis of the metabolic flexibility of *Galdieria sulphuraria* and significant differences in carbohydrate metabolism of both algae. *Plant Physiol.* **2005**, *137*, 460–474. [[PubMed](#)]
10. Yu, S. Enzymes of floridean starch and floridoside degradation in red algae: Purification, characterization and physiological studies. *Acta Univ. Ups.* **1992**, *372*, 1–47.
11. Yu, S.; Pedersén, M. The  $\alpha$ -galactosidase of *Gracilaria tenuistipitata* and *G. sordida* (Gracilariales, Rhodophyta). *Phycologia* **1990**, *29*, 454–460. [[CrossRef](#)]
12. Lee, W.K.; Lim, Y.Y.; Leow, A.T.C.; Namasivayam, P.; Abdullah, J.O.; Ho, C.L. Biosynthesis of agar in red seaweeds: A review. *Carbohydr. Polym.* **2017**, *164*, 23–30. [[CrossRef](#)]
13. Raymond, J.A.; Morgan-Kiss, R.; Stahl-Rommel, S. Glycerol is an osmoprotectant in two antarctic *Chlamydomonas* species from an ice-covered saline lake and is synthesized by an unusual bidomain enzyme. *Front. Plant Sci.* **2020**, *11*, 1259. [[CrossRef](#)]
14. Robaina, R.R.; Garcia-Jimenez, P.; Garcia-Reina, G.; Luque, A. Morphogenetic effect of glycerol on tissue cultures of the red seaweed *Grateloupia doryphora*. *J. Appl. Phycol.* **1990**, *2*, 137–143. [[CrossRef](#)]
15. Lin, H.; Fang, L.; Low, C.S.; Chow, Y.; Lee, Y.K. Occurrence of glycerol uptake in *Dunaliella tertiolecta* under hyperosmotic stress. *FEBS J.* **2013**, *280*, 1064–1072. [[CrossRef](#)]
16. Yuzawa, Y.; Nishihara, H.; Haraguchi, T.; Masuda, S.; Shimojima, M.; Shimoyama, A.; Yuasa, H.; Okada, N.; Ohta, H. Phylogeny of galactolipid synthase homologs together with their enzymatic analyses revealed a possible origin and divergence time for photosynthetic membrane biogenesis. *DNA Res.* **2012**, *19*, 91–102. [[CrossRef](#)]
17. Yu, C.W.; Lin, Y.T.; Li, H.M. Increased ratio of galactolipid MGDG: DGDG induces jasmonic acid overproduction and changes chloroplast shape. *New Phytol.* **2020**, *228*, 1327–1335. [[CrossRef](#)]
18. Yu, L.; Zhou, C.; Fan, J.; Shanklin, J.; Xu, C. Mechanisms and functions of membrane lipid remodeling in plants. *Plant J.* **2021**, *107*, 37–53. [[CrossRef](#)]
19. Goulard, F.; Diouris, M.; Quere, G.; Deslandes, E.; Flocaos, J.Y. Salinity effects on NDP-sugars, floridoside, starch, and carrageenan yield, and UDP-glucose-pyrophosphorylase and-epimerase activities of cultivated *Solieria chordalis*. *J. Plant Physiol.* **2001**, *158*, 1387–1394. [[CrossRef](#)]
20. Siow, R.-S.; Teo, S.-S.; Ho, W.-Y.; Shukor, M.Y.A.; Phang, S.-M.; Ho, C.-L. Molecular cloning and biochemical characterization of galactose-1-phosphate uridylyltransferase from *Gracilaria changii* (Rhodophyta). *J. Phycol.* **2021**, *48*, 155–162. [[CrossRef](#)] [[PubMed](#)]
21. Garcia-Jimenez, P.; Robaina, R.R.; Montero-Fernández, M. Molecular mechanisms underlying *Grateloupia imbricata* (Rhodophyta) carposporogenesis induced by methyl jasmonate. *J. Phycol.* **2017**, *53*, 1340–1344. [[CrossRef](#)] [[PubMed](#)]
22. McQueney, M.S.; Anderson, K.S.; Markham, G.D. Energetics of S-adenosylmethionine synthetase catalysis. *Biochemistry* **2000**, *39*, 4443–4454. [[CrossRef](#)] [[PubMed](#)]
23. Norbeck, J.; Pålman, A.K.; Akhtar, N.; Blomberg, A.; Adler, L. Purification and characterization of two isoenzymes of DL-glycerol-3-phosphatase from *Saccharomyces cerevisiae*: Identification of the corresponding GPP1 and GPP2 genes and evidence for osmotic regulation of Gpp2p expression by the osmosensing mitogen-activated protein kinase signal transduction pathway. *J. Biol. Chem.* **1996**, *271*, 13875–13881.
24. Koornneef, A.; Leon-Reyes, A.; Ritsema, T.; Verhage, A.; Den Otter, F.C.; Van Loon, L.C.; Pieterse, C.M.J. Kinetics of salicylate-mediated suppression of jasmonate signaling reveal a role for redox modulation. *Plant Physiol.* **2008**, *147*, 1358–1368. [[CrossRef](#)] [[PubMed](#)]
25. Driver, T.; Trivedi, D.K.; McIntosh, O.A.; Dean, A.P.; Goodacre, R.; Pittman, J.K. Two glycerol-3-phosphate dehydrogenases from *Chlamydomonas* have distinct roles in lipid metabolism. *Plant Physiol.* **2017**, *174*, 2083–2097. [[CrossRef](#)]
26. Ansell, R.; Granath, K.; Hohmann, S.; Thevelein, J.M.; Adler, L. The two isoenzymes for yeast NAD<sup>+</sup>-dependent glycerol 3-phosphate dehydrogenase encoded by GPD1 and GPD2 have distinct roles in osmoadaptation and redox regulation. *EMBO J.* **1997**, *16*, 2179–2187. [[CrossRef](#)] [[PubMed](#)]
27. Lai, X.J.; Yang, R.; Luo, Q.J.; Chen, J.J.; Chen, H.M.; Yan, X.J. Glycerol-3-phosphate metabolism plays a role in stress response in the red alga *Pyropia haitanensis*. *J. Phycol.* **2015**, *51*, 321–331. [[CrossRef](#)]
28. Miller, G.; Suzuki, N.; Ciftci-Yilmaz, S.; Mittler, R. Reactive oxygen species homeostasis and signaling during drought and salinity stresses. *Plant Cell Environ.* **2010**, *33*, 453–467. [[CrossRef](#)]

29. Weinberger, F.; Lion, U.; Delage, L.; Kloareg, B.; Potin, P.; Beltran, J.; Flores, V.; Faugeron, S.; Correa, J.; Pohnert, G. Up-regulation of lipoxygenase, phospholipase, and oxylipin-production in the induced chemical defense of the red alga *Gracilaria chilensis* against epiphytes. *J. Chem. Ecol.* **2011**, *33*, 677–686. [[CrossRef](#)]
30. Higashi, Y.; Okazaki, Y.; Myouga, F.; Shinozaki, K.; Saito, K. Landscape of the lipidome and transcriptome under heat stress in *Arabidopsis thaliana*. *Sci. Rep.* **2015**, *5*, 10533. [[CrossRef](#)]
31. Yuan, L.; Mao, X.; Zhao, K.; Ji, X.; Ji, C.; Xue, J.; Li, R. Characterisation of phospholipid: Diacylglycerol acyltransferases (PDATs) from *Camelina sativa* and their roles in stress responses. *Biol. Open* **2017**, *6*, 1024–1034.
32. Luo, S.; Levine, R.L. Methionine in proteins defends against oxidative stress. *FASEB J.* **2009**, *23*, 464–472. [[CrossRef](#)]
33. Garcia-Jimenez, P.; Brito-Romano, O.; Robaina, R.R. Production of volatiles by the red seaweed *Gelidium arbuscula* (Rhodophyta): Emission of ethylene and dimethyl sulfide. *J. Phycol.* **2013**, *49*, 661–669. [[CrossRef](#)] [[PubMed](#)]
34. André, L.; Hemming, A.; Adler, L. Osmoregulation in *Saccharomyces cerevisiae* studies on the osmotic induction of glycerol production and glycerol 3-phosphate dehydrogenase (NAD<sup>+</sup>). *FEBS Lett.* **1991**, *286*, 13–17. [[CrossRef](#)] [[PubMed](#)]
35. Ericksson, P.; Andre, L.; Ansell, R.; Blomberg, A.; Adler, L. Molecular cloning of GPD2, a second gene encoding sn-glycerol-3-phosphate dehydrogenase (NAD<sup>+</sup>) in *Saccharomyces cerevisiae*. *Mol. Microbiol.* **1995**, *17*, 95–107. [[CrossRef](#)] [[PubMed](#)]
36. Guo, Q.; Liu, L.; Barkla, B.J. Membrane lipid remodeling in response to salinity. *Int. J. Mol. Sci.* **2019**, *20*, 4264. [[CrossRef](#)] [[PubMed](#)]
37. Reed, R.H.; Collins, J.C.; Russell, G. The effects of salinity upon galactosyl-glycerol content and concentration of the marine red alga *Porphyra purpurea* (Roth) C. Ag. *J. Exp. Bot.* **1980**, *31*, 1539–1554. [[CrossRef](#)]
38. Kirst, G.O. Low molecular weight carbohydrates and ions in Rhodophyceae: Quantitative measurement of floridoside and digeneaside. *Phytochemistry* **1980**, *19*, 1107–1110. [[CrossRef](#)]
39. Ekman, P.; Yu, S.; Pedersen, M. Effects of altered salinity, darkness and algal nutrient status on floridoside and starch content,  $\alpha$ -galactosidase activity and agar yield of cultivated *Gracilaria sordida*. *Brit. Phycol. J.* **1991**, *26*, 123–131. [[CrossRef](#)]
40. Arunraj, R.; Skori, L.; Kumar, A.; Hickerson, N.M.; Shoma, N.; Samuel, M.A. Spatial regulation of alpha-galactosidase activity and its influence on raffinose family oligosaccharides during seed maturation and germination in *Cicer arietinum*. *Plant Signal. Behav.* **2020**, *15*, 1709707. [[CrossRef](#)]
41. Giordano, M.; Raven, J.A. Nitrogen and sulfur assimilation in plants and algae. *Aquat. Bot.* **2014**, *118*, 45–61. [[CrossRef](#)]
42. Garcia-Jimenez, P.; Montero-Fernández, M.; Robaina, R.R. Analysis of ethylene-induced gene regulation during carposporogenesis in the red seaweed *Grateloupia imbricata* (Rhodophyta). *J. Phycol.* **2018**, *54*, 681–689. [[CrossRef](#)] [[PubMed](#)]

**Disclaimer/Publisher's Note:** The statements, opinions and data contained in all publications are solely those of the individual author(s) and contributor(s) and not of MDPI and/or the editor(s). MDPI and/or the editor(s) disclaim responsibility for any injury to people or property resulting from any ideas, methods, instructions or products referred to in the content.